IEEE Access
Multidisciplinary ⋮ Rapid Review ⋮ Open Access Journal

IEEE POWER & ENERGY SOCIETY SECTION

Received 13 May 2025, accepted 31 May 2025, date of publication 9 June 2025, date of current version 16 June 2025.

Digital Object Identifier 10.1109/ACCESS.2025.3577987

RESEARCH ARTICLE

Pole Slipping in Droop-Based Grid-Forming Inverters

NEGAR KARIMIPOUR[1], (Member, IEEE),
HANSI WIJAYALATH ARACHCHILAGE[2], (Graduate Student Member, IEEE),
AMIR ABIRI JAHROMI[3], (Senior Member, IEEE),
BEHROOZ BAHRANI[2], (Senior Member, IEEE),
AND MOHAMMADREZA F. M. ARANI[1], (Member, IEEE)
[1]Department of Electrical, Computer, and Biomedical Engineering, Toronto Metropolitan University, Toronto, ON M5B 2K3, Canada
[2]Department of Electrical and Computer Systems Engineering, Monash University, Clayton, VIC 3800, Australia
[3]School of Electronic and Electrical Engineering, University of Leeds, LS2 9JT Leeds, U.K.

Corresponding author: Negar Karimipour (nkarimipour@torontomu.ca)

This work was supported by the Natural Sciences and Engineering Research Council of Canada under Grant RGPIN-2020-04645.

ABSTRACT Integration of grid-forming inverter-based resources is considered as a viable solution to address the challenges associated with the dynamics of power systems with high penetration levels of inverter-based resources. Yet, various aspects of dynamic behaviour of grid-forming inverters during disturbances have remained unknown. This paper for the first time introduces the concept of pole slipping in grid forming inverters, referring to the loss of synchronism where the inverter's internal phase angle deviates beyond 180° with respect to the grid, similar to synchronous generators losing step. It is revealed that this event in grid forming inverters can be stable or unstable. The differences between stable and unstable pole slipping are highlighted. The determining factors for the occurrence of stable and unstable pole slipping in grid forming inverters and equipment-level implications of pole slipping are identified and studied. A solution is proposed to mitigate stable and unstable pole slipping in grid-forming inverters by adjusting the operating reference power during the disturbance. The validity of the proposed concept of pole slipping in grid forming inverters and the proposed solution is tested and verified through extensive time-domain simulations and experimental results. The results verify that pole slipping is more likely to happen in high short circuit ratios (SCRs). It is revealed that unstable pole slipping does not occur at SCRs lower than 3.5. Simulation and experimental results demonstrate that a phase jump as small as 10° may lead to instability in a grid with SCRs equal or higher than 10. This is while in lower SCRs such phase jumps result in long fault recovery without causing pole slipping.

INDEX TERMS Droop-based grid-forming inverters, pole slipping, circular current limiter, transient stability.

I. INTRODUCTION

Electric power systems are undergoing a rapid transformation as inverter-based clean energy resources increasingly replace fossil fuel-based synchronous generators [1]. Among these clean energy resources, grid-following inverter-based resources (GFL-IBRs) dominate current installations. Unlike synchronous generators, GFL-IBRs inherently lack the capability for voltage and frequency regulation, which leads to a deterioration in power system dynamics as their penetration increases [2], [3]. Furthermore, GFL-IBRs rely on phase-locked loops (PLLs) for synchronization with the grid, a mechanism that makes them particularly prone to instability in weak grid scenarios [4], [5].

To address these challenges, *grid-forming inverter-based resources (GFM-IBRs)* have emerged as a promising solution to enhance the stability of low-carbon power systems. GFM-IBRs emulate the behavior of synchronous generators by regulating voltage and frequency while also eliminating the challenges associated with PLL-based synchronization [6]. However, the current output of GFM-IBRs is typically restricted to 1.2 per unit (pu), unlike synchronous generators

The associate editor coordinating the review of this manuscript and approving it for publication was Suman Maiti.

that can deliver fault currents exceeding seven pu. This limited fault current capability poses challenges for transient stability and protection in power systems [7], [8].

The dynamic behavior of GFM-IBRs during disturbances has been the focus of significant research in recent years. Some studies have explored GFM-IBRs performance under various fault conditions, investigating the impact of fault type and severity on system stability [9], [10], [11], [12]. In [13], a strategy has been proposed to mitigate instability during transitions from voltage control to current control. A methodology for optimizing current reference angles to enhance transient stability has been presented in [14]. Advanced current limiter designs have been introduced in [15] and [16] to improve fault recovery. Furthermore, the stability of GFM-IBRs equipped with circular current limiters has been analyzed in [17]. Chetaev's instability theorem has been employed to derive instability conditions. Enhanced droop-based control strategies and equivalent circuit models have been developed in [18] and [19] for transient stability analysis of GFM-IBRs.

While existing studies provide valuable insights into GFM-IBR stability under voltage drops, various aspects of the transient response of grid-forming inverters during disturbances have remained unexplored. The majority of existing studies neglect the combined effects of voltage phase angle jumps and voltage drops which are common occurrences in transmission systems during disturbances as discussed in [20], [21], and [22]. In particular, the effect of voltage phase angle jump on the transient stability of GFM-IBRs has received little attention. The inverter power angle stability issues often resemble rotor angle stability problems in traditional power systems, commonly known as *pole slipping* or *power swing* [23]. Pole slipping occurs when the rotor angle of a synchronous generator consistently varies with respect to the rest of the system under disturbances, potentially leading to instability, voltage depression, reverse power flow, and misoperation of protection devices [23], [24]. Despite the critical importance of pole slipping in power systems, this phenomenon in GFM-IBRs has not been thoroughly investigated.

This paper addresses this gap by introducing, for the first time, the concept of *pole slipping in GFM-IBRs*, including those equipped with circular current limiters. To be more specific, *pole slipping* in grid-forming inverters refers to the loss of synchronism where the inverter's internal phase angle deviates beyond 180° with respect to the grid, similar to synchronous generators losing step. The conditions for stable and unstable pole slipping in GFM-IBRs are derived, and the factors influencing this phenomenon are identified and analyzed. Additionally, the paper discusses the equipment-level challenges posed by pole slipping, such as overvoltage, reverse power flow, and overloading, and proposes a novel control strategy to mitigate these effects. This solution is validated through comprehensive time-domain simulations and experimental results, offering a framework for evaluating transient stability in GFM-IBRs under both voltage drops and phase angle jumps.

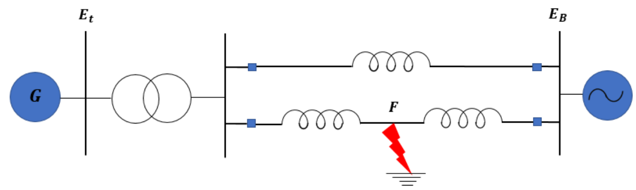

FIGURE 1. Single machine infinite bus model.

The primary contributions of this paper are as follows:

- The concept of *pole slipping* in GFM-IBRs is introduced and analyzed, with distinctions drawn between stable and unstable pole slipping.
- The determining factors for the occurrence of pole slipping in GFM-IBRs are identified, and the implications for stability and protection are discussed.
- A novel control strategy is proposed to prevent both stable and unstable pole slipping, addressing the limitations of existing voltage-based methods.
- The impact of phase angle jumps on GFM-IBRs is thoroughly investigated, demonstrating that even small phase angle jumps can induce pole slipping.

The remainder of the paper is structured as follows. Section II introduces the concept of pole slipping in GFM-IBRs, along with the factors influencing its occurrence. Section III presents a transient stability analysis to derive the conditions for stable and unstable pole slipping. Section IV outlines the proposed mitigation strategy. Section V provides time-domain simulation results, including a comparison of the proposed solution with an existing voltage-based method. The experimental validations of the concept and the proposed method are presented in Section VI. Section VII concludes the paper and provides future research directions.

II. POLE SLIPPING

A. POLE SLIPPING IN SYNCHRONOUS GENERATORS

Transient disturbances such as faults can cause an imbalance between the mechanical power input and electrical power output of a synchronous generator. This power imbalance can cause rotor angle instability in a synchronous generator.

The equal area criterion is commonly used in power systems to analyze rotor angle stability [25]. Fig. 1 demonstrates the classic single machine infinite bus model. Moreover, the electric power-angle curve of a synchronous generator is shown in Fig. 2.

After the occurrence of a fault on the transmission line as illustrated in Fig. 1, the power transfer capability of the transmission system reduces. Thus, the operating point of the synchronous generator moves from point a to point b in Fig. 2. As the electric power output is lower than the mechanical power input in point b, the rotor angle of the synchronous generator accelerates and the rotor angle moves to point c. When the fault clears, the electrical power output of the synchronous generator increases and the

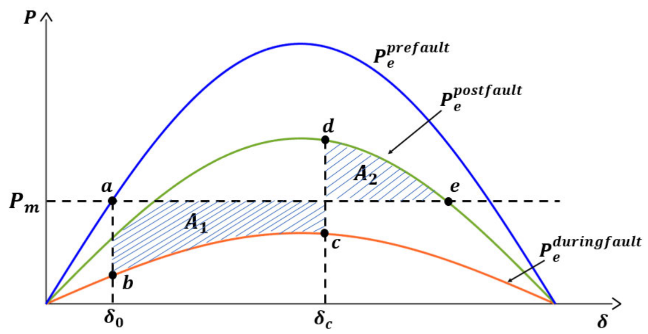

FIGURE 2. Power-angle relationship for a synchronous generator.

operating point moves to point d. At this point, the mechanical power output is smaller than the electrical power output. Therefore, the rotor speed of the synchronous generator decreases. However, the rotor angle continues to increase to point e. If area A1 in Fig. 2 is equal to or smaller than area A2, the generator maintains synchronism. Otherwise, the synchronous generator loses synchronism.

If the balance between the mechanical power input and the electrical power output of the synchronous generator is restored, a new stable operating point will be established and the synchronism will be attained. Otherwise, the rotor angle will increase and the synchronous generator slips a pole, which is also referred to as an *out-of-step* condition in the literature. Pole slipping is a condition whereby the rotor angle of a synchronous generator goes beyond 180 degrees with respect to the rest of the power system.

Pole slipping is potentially damaging to synchronous generators. The synchronous generator pole slipping can further cause oscillations in other parts of the system. This is well-studied in protection studies considering out-of-step and power swing blocking relays [26], [27], [28]. In practice, it is commonly recommended to disconnect the synchronous generators when the critical angle for maintaining stability is reached without any delay. It is worth noting that some hydro unit operators may practice to separate their unit only after it experiences a certain number of pole slips. This is because a hydro unit possibly can get back into synchronism after pole slipping [29].

In the next section, we present a phenomenon in grid-forming voltage source converters similar to pole slipping in synchronous generators.

B. POLE SLIPPING IN DROOP-BASED GFM-IBRS WITH CURRENT LIMITING FAULT RIDE THROUGH MECHANISM

Disturbances such as faults, transmission line switching, and generation/load connections/disconnections can cause an imbalance between the active power reference (P_{ref}) and active power output (P_{inv}) of a droop-based GFM inverter analogous to synchronous generators. Fig. 3 demonstrates the single machine infinite bus model for a GFM inverter. The synchronizing equation of a droop-based GFM inverter is given in (1).

$$\omega - \omega_0 = m_p \frac{\omega_{\text{pcf}}}{s + \omega_{\text{pcf}}}(P_{\text{ref}} - P_{\text{inv}}) \tag{1}$$

where ω, ω_0 and ω_{pcf} denote angular frequency of the inverter, nominal frequency, and low-pass filter cut-off frequency, respectively. m_p denotes the droop gain.

The P_{inv} of a droop-based GFM inverter with a circular current limiter is given in (2). The derivation of (2) is provided in the Appendix. The derivation of (2) is based on [19] where a droop-based GFM inverter with a circular current limiter is modelled by a voltage source behind an equivalent non-negative resistance. It is worth noting that the resistance r_e in the model is a state dependent parameter. Although droop-based GFM with non-priority circular current limiter is considered here, the proposed notions can be extended to other current limiting methods as well.

$$\begin{aligned} P_{\text{inv}} = \frac{3}{2}\left[\frac{(r_e + r_g)(V_{\text{ref}}^2 - V_{\text{ref}}V_g\cos(\delta - \theta_g))}{(r_e + r_g)^2 + \omega_g^2 l_g^2}\right] \\ - \frac{3}{2}\left[r_e I_{\text{th}}^2 + \frac{\omega_g l_g V_{\text{ref}} V_g \sin(\delta - \theta_g))}{(r_e + r_g)^2 + \omega_g^2 l_g^2)}\right] \end{aligned} \tag{2}$$

where r_e and r_g denote equivalent resistance and grid resistance, respectively. l_g denotes grid inductance. ω_g denotes grid angular frequency. V_g and V_{ref} denote grid voltage magnitude and voltage reference, respectively. I_{th} denotes the maximum allowable converter current magnitude. δ and θ_g denote power angle and grid voltage angle, respectively.

Furthermore, δ in (2) is given in (3).

$$\dot{\delta} = \omega - \omega_0 \tag{3}$$

An approach similar to the equal area method is adopted here to analyze the power angle behavior of GFM inverters. The impact of voltage drop without voltage phase angle jump on the power-angle behavior of GFM inverters has been previously examined and solutions have been proposed [8], [14], [17], [18], [30], [31], [32]. However, the impact of disturbance-induced voltage phase angle jumps on power angle stability of GFM inverters has rarely been investigated in the literature [14], [33]. This paper, for the first time, not only examines the impact of voltage phase angle jumps on the power angle behavior of droop-based GFM inverters, but also provides a solution to improve the power angle behavior. In order to avoid overly complicated analyses and develop insight, we discuss the case of voltage phase angle jump without voltage drop in the following. However, the simulation results cover the general case when a combination of voltage drop and voltage phase angle jump occurs due to a disturbance.

The imbalance between the active power output and active power reference of an inverter due to disturbance-induced voltage phase angle jumps can produce three outcomes; 1) restoration to a stable point without pole slipping, 2) restoration to a stable point after pole slipping, and 3) unstable pole slipping. Fig. 4 demonstrates the

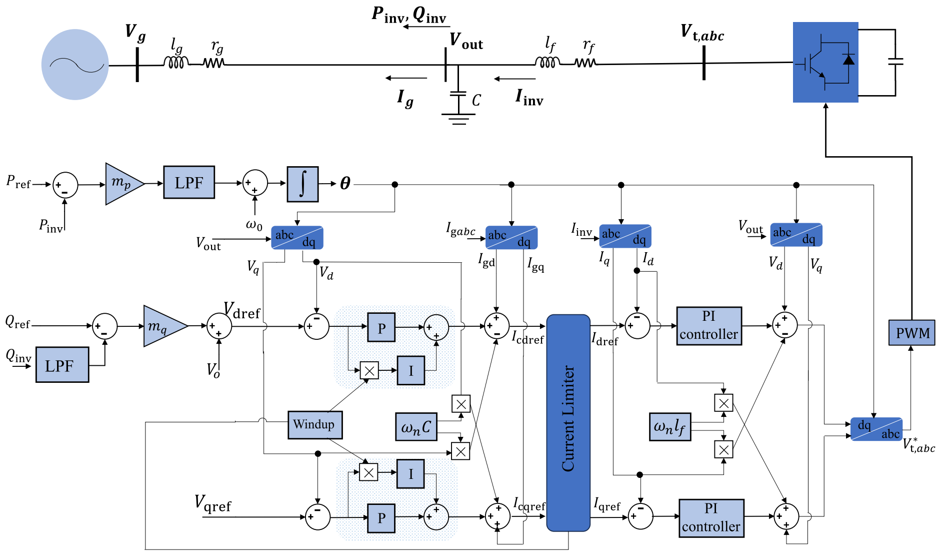

FIGURE 3. GFM-IBR connected to an infinite bus (SMIB) model and its control structure.

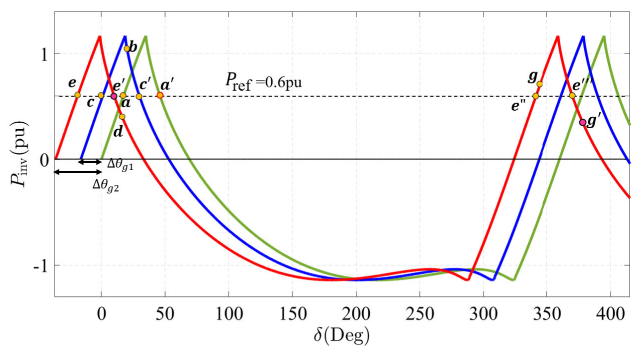

FIGURE 4. Power-angle relationship for a GFM-IBR with a circular current limiter.

power-angle curve of an inverter for the abovementioned three cases which are discussed in the following sections.

1) RESTORATION TO A STABLE OPERATING POINT WITHOUT POLE SLIPPING

After the occurrence of voltage phase angle jump without voltage drop at the terminal of an inverter, the power-angle curve of the inverter shifts from the green curve to the blue curve on the left as illustrated in Fig. 4. Thus, the operating point of the inverter moves from point a to point b in Fig. 4. As the active power output of the inverter is higher than the active power reference in point b, the power angle of the inverter decreases and the operating point restores to the stable operating point at c.

2) STABLE POLE SLIPPING

In this case, the power-angle curve of the inverter shifts from the green curve to the red curve on the left as illustrated in Fig. 4 due to the occurrence of voltage phase angle jump. Thus, the operating point of the inverter moves from point a to point d in Fig. 4. As the active power output of the inverter is lower than the active power reference in point d, the power angle of the inverter increases and the operating point moves to the operating point at e''. However, the inverter power angle continues to increase to point g where $\omega = \omega_0$. At point g, the active power reference is less than the active power output. Therefore, the power angle decreases and settles at the stable operating point e''. As illustrated in Fig. 4, the pole slipping occurs in this case. Thus, the new operating point is at point e'' instead of point e.

The characteristics of critical voltage phase angle jump that determine whether the inverter experiences pole slipping or not is discussed here. As illustrated in Fig. 4, each power-angle curve of the inverter has a stable and an unstable equilibrium point in $(-180°, 180°)$. For instance, points e (c) and e' (c') on the red curve (blue curve) illustrate the stable and unstable equilibrium points, respectively. After the occurrence of voltage phase angle jump, the power angle of the inverter does not change immediately. However, the two equilibrium points shift to the left with an amount equal to voltage phase angle jump. If the absolute value of the voltage phase angle jump is larger than the critical voltage phase angle jump, the angle of the new unstable equilibrium point, e.g. e', is less than the power angle of the operating point right before the disturbance. Thus, pole slipping takes place. Otherwise, the angle of the new unstable equilibrium point, e.g. c', is larger than the power angle of the operating point right before the disturbance. Therefore, the operating point restores to a new stable equilibrium point without pole slipping. The critical voltage phase angle jump in the absence of voltage drop is equal to the phase angle difference between the stable and unstable equilibrium points.

3) UNSTABLE POLE SLIPPING

In this case, the power-angle curve of the inverter shifts from the green curve to the red curve in Fig. 4 similar to the

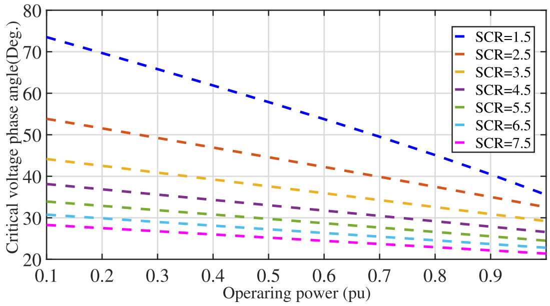

FIGURE 5. Critical voltage phase angle jump that leads to pole slipping at different operating points of the GFM-IBR.

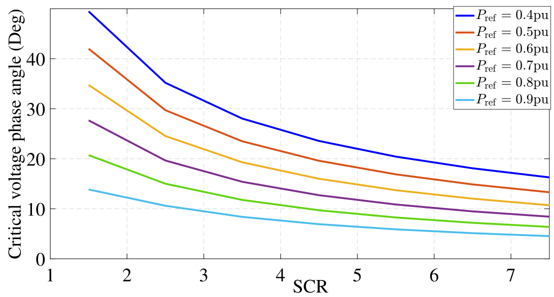

FIGURE 6. Critical voltage phase angle jump that leads to pole slipping at different grid strengths.

stable pole slipping case due to the occurrence of voltage phase angle jump. However, the operating point moves to the operating point g' instead of point g where $\omega = \omega_0$. Beyond point e''', the active power reference is larger than the active power output. Therefore, the power angle increases again and the inverter experiences one pole slipping after another. As such, the power angle of the inverter becomes unstable.

C. INFLUENCING FACTORS ON POLE SLIPPING IN GFM-IBRS

The critical voltage phase angle jump that leads to pole slipping depends both on the short circuit ratio (SCR) of the grid and the operating point of the inverter before the disturbance. Fig. 5 illustrates the critical voltage phase angle jumps for different operating points. As illustrated in Fig. 5, the critical voltage phase angle jumps that can cause pole slipping becomes smaller when the inverter operates at higher active power output. However, the dependence of the critical voltage phase angle jump on the operating point of the inverter decreases when the SCR of the grid increases. It is worth noting that voltage phase angle jumps as small as 10° can cause pole slipping in GFM-IBRs as illustrated in Fig. 5. As such, even small voltage phase angle jumps created by disturbances can cause pole slipping in GFM-IBRs.

Fig. 6 illustrates the critical voltage phase angle jumps for different SCRs. As illustrated in Fig. 6, smaller voltage phase angle jumps can cause pole slipping at higher SCRs. Thus, the risk of pole slipping in inverters is higher in stiff grids which is counter intuitive. It is worth noting that voltage phase angle jump due to disturbances is smaller in stiff grids compared to weak grids. Fig. 6 further indicates that the critical voltage phase angle jump may vary by changes in the configuration of the network. This creates new challenges for the dynamic behaviour of GFM-IBRs based on different grid configurations.

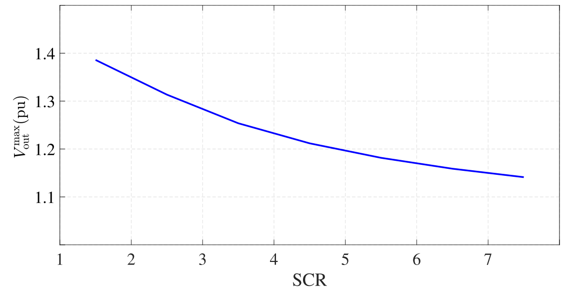

FIGURE 7. Maximum inverter voltage during pole slipping at different grid strengths.

The critical voltage phase angle jump illustrated in Figs. 5 and 6 determines the occurrence of pole slipping, but further analysis is needed to determine whether pole slipping is stable or unstable. This is examined in the following sections.

D. CHALLENGES INTRODUCED BY POLE SLIPPING IN GFM-IBRS

Stable and unstable pole slipping in GFM-IBRs have equipment-level and system-wide implications for power systems which makes it completely different from stability analysis. This paper focuses on equipment-level implications of pole slipping. Pole slipping of inverters can cause serious challenges for power systems such as reverse power flow. As illustrated in Fig. 4, the power output of an inverter can become negative during pole slipping before settling in the new operating point at e''. This phenomenon is similar to pole slipping in synchronous generators. The magnitude of the reverse power flow in inverters due to pole slipping can be as high as 1.2 pu. The reverse power flow can be handled by resources like energy storage but can be damaging to other resources such as type-IV wind generators.

Pole slipping of inverters can further cause an overvoltage in the grid. As illustrated in Fig. 7, the maximum overvoltage that can be caused by pole slipping have reverse relationship with the SCR of the grid. The maximum overvoltage can exceed 1.2 pu in SCRs lower than 4.85. This overvoltage level is important as it may trigger the overvoltage relay and trip the inverter [34], [35]. As such, even stable pole slipping is undesirable in these cases as it can create undesirable overvoltage and should be prevented. A solution to this problem is proposed in Section IV.

Furthermore, unstable pole slipping may cause overheating of the inverter switches. As illustrated in Fig. 8, the overheating of inverter switches may occur in unstable pole slipping because the inverter supplies the maximum current continually in each pole slip.

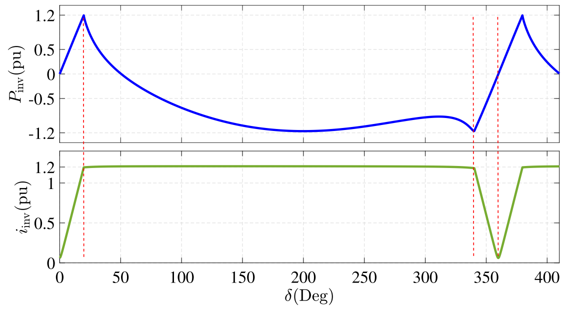

FIGURE 8. Current-angle relationship for a GFM-IBR with a circular current limiter.

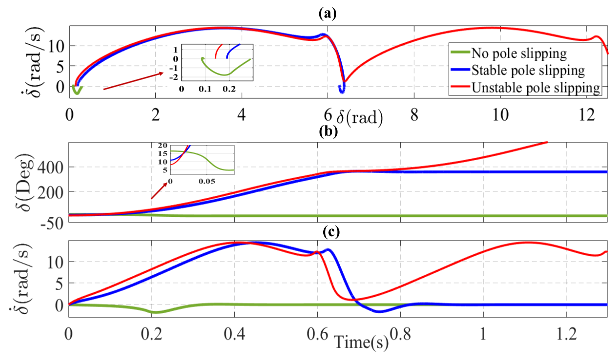

FIGURE 9. Phase portrait and the numerical solutions for transient stability of GFM-IBR.

III. TRANSIENT STABILITY ANALYSIS

In this section, the nonlinear ordinary differential equations describing the transient stability of the GFM-IBRs are solved numerically to determine whether pole slipping of the inverter is stable or unstable. We begin by reordering the synchronizing and active power output equations of the GFM-IBR in (1) and (2) as given in (4)-(6).

$$y_1 = \delta \tag{4}$$

$$y_2 = \dot{y_1} \tag{5}$$

$$\dot{y_2} = -\omega_{\text{pcf}} y_2 + m_p \omega_{\text{pcf}} P_{\text{ref}} - m_p \omega_{\text{pcf}} P_{\text{inv}} \tag{6}$$

Power angle (δ) and the change in the angular frequency of the inverter ($\dot{\delta}$) in (4) and (5) are calculated by applying the fourth-order Runge-Kutta method to (4)-(6). Fig. 9 illustrates the numerical solutions for three possible cases: 1) restoration to a stable operating point without pole slipping, 2) restoration to a stable operating point after pole slipping, and 3) unstable pole slipping. As illustrated in Fig. 9 by green curve, the power angle decreases to a new stable equilibrium point when there is no pole slipping. In the case of stable pole slipping, the power angle increases more than π radians (180°), as shown by the blue curve in Fig. 9, before settling to a new stable equilibrium point where $\dot{\delta} = 0$. In the case of unstable pole slipping, the power angle increases continually, as shown by red curve in Fig. 9, without settling to a stable equilibrium point. Thus, the condition $\dot{\delta} = 0$ can be used to distinguish stable pole slipping from unstable pole slipping.

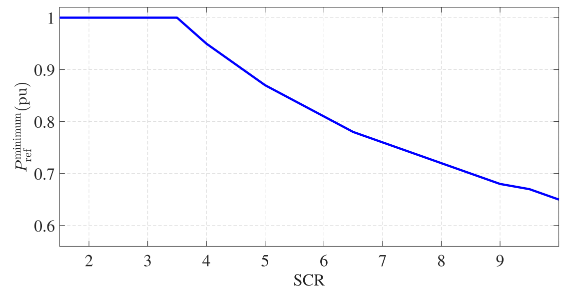

FIGURE 10. Minimum active power output that can cause unstable pole slipping at different grid strengths.

TABLE 1. Minimum Active Power Leading to Unstable Pole Slipping.

m_p(pu)	ω_{pcf}(pu)	$P_{\text{ref}}^{\text{minimum}}$		
		SCR=3	SCR=6	SCR=9
0.01	0.10	0.98	0.98	0.91
0.02	0.10	0.98	0.78	0.66
0.03	0.10	0.85	0.62	0.51
0.04	0.10	0.75	0.62	0.41
0.02	0.03	0.30	0.28	0.19
0.02	0.05	0.74	0.53	0.43
0.02	0.08	0.92	0.69	0.57
0.02	0.11	0.98	0.80	0.67

The condition $\dot{\delta} = 0$ is used to numerically obtain Fig. 10 which shows the impact of the operating point and SCR on determining the stable and unstable pole slipping. As illustrated in Fig, 10, unstable pole slipping does not occur at SCRs lower than 3.5. The minimum active power output that can cause pole slipping decreases as the SCR grows. For example, active power outputs higher than 0.65 pu causes unstable pole slipping for SCRs equal or larger than 10. As discussed in Section II, critical voltage phase angle jumps decreases at high SCRs. Therefore, even small voltage phase angle jumps created by disturbances can cause unstable pole slipping in GFM-IBRs.

Droop-gain (m_p) and cut-off frequency of droop low-pass filter (ω_{pcf}) are the influencing factors for determining whether stable or unstable pole slipping occurs. Table 1 summarizes the results of the analysis on how these two factors influence the stability of GFM-IBRs during a disturbance. Minimum P_{ref} in pu for different ω_{pcf} and m_p are provided in the table. Unstable pole slipping happens if the reference active power of the droop controller exceeds these critical values. As mentioned earlier, the critical reference power changes when SCR increases. In addition, by decreasing droop gain, the possibility of unstable pole slipping reduces, but it cannot prevent stable pole slipping. Moreover, increasing the cut-off frequency of the droop low-pass filter enhances the power angle stability of the inverter. It is worth noting that by ignoring the droop low-pass filter in the models, the unstable pole slipping will not be observed. This underlines the importance of modeling the droop low-pass filter in transient stability studies of GFM-IBRs.

IV. PROPOSED SOLUTION

Pole slipping occurs in droop-based GFM-IBRs when the following two conditions hold: 1) the power angle of the inverter is larger than the power angle of the closest stable equilibrium point, and 2) the active power output (P_{inv}) of the inverter is less than the active power reference (P_{ref}). The second condition forces the synchronism mechanism of the inverter to increase the power angle to the point where the balance between P_{inv} and P_{ref} is restored. This creates pole slipping. As such, pole slipping in GFM-IBRs can be prevented by eliminating condition 2.

In order to remove condition 2, we propose to modify the active power reference during the disturbance as given in (7). By modifying the active power reference during the disturbance, the equilibrium between P_{ref} and P_{inv} can be achieved without the need to increase the power angle.

$$P_{ref}^{disturbance} = P_{ref} - P_{add} \tag{7}$$

P_{add} in (7) must satisfy the condition in (8) to prevent pole slipping.

$$P_{add} > P_{ref} - P_{inv} \tag{8}$$

The proposed P_{add} is given in (9). It is worth noting that P_{add} does not intervene with the synchronism mechanism of the inverter in normal operating conditions because it is equal to zero. P_{add} becomes non-zero by the activation of the current limiter irrespective of the source of the disturbance.

$$P_{add} = k r_e I_{th}^2 \tag{9}$$

where r_e denotes equivalent resistance which depends on δ. I_{th} denotes the maximum allowable converter current magnitude. k in (9) must be chosen such that it satisfies (10). Inequality (10) is derived by replacing (9) in (8).

$$k > \frac{P_{ref} - P_{inv}}{r_e I_{th}^2} = f(\delta) \tag{10}$$

$$\begin{aligned} f(\delta) = {} & \frac{P_{ref}}{r_e I_{th}^2} - \frac{3}{2}\left[\frac{(r_e + r_g)(V_{ref}^2 - V_{ref}V_g\cos(\delta))}{((r_e + r_g)^2 + \omega_g^2 l_g^2) r_e I_{th}^2}\right] \\ & - \frac{3}{2}\left[1 + \frac{\omega_g l_g V_{ref} V_g \sin(\delta))}{((r_e + r_g)^2 + \omega_g^2 l_g^2) r_e I_{th}^2}\right] \end{aligned} \tag{11}$$

Inequality (10) is satisfied for any value of δ when k is larger than the maximum value of $f(\delta)$ in (11). The maximum value of $f(\delta)$ can be calculated using numerical methods. It is worth noting that P_{ref} should be equal to one when calculating k to ensure k is valid for all the operating points of the inverter. Moreover, the maximum value of $f(\delta)$ is only calculated for the practical range of δ.

The reason why P_{add} is proportional to k, r_e, and I_{th}^2 is as follows:

- r_e is considered because it reflects the severity of the disturbance. More severe disturbances produces larger r_e as described in the Appendix. Moreover, r_e is zero in the absence of a disturbance and forces P_{add} to become zero in the absence of a disturbance.
- I_{th}^2 is considered to convert r_e to power.
- Lastly, k is considered to ensure that the proposed P_{add} works for a wide range of disturbances and SCR values.

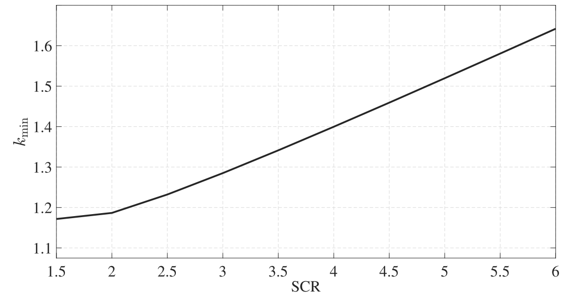

FIGURE 11. Minimum value of k at different grid strengths.

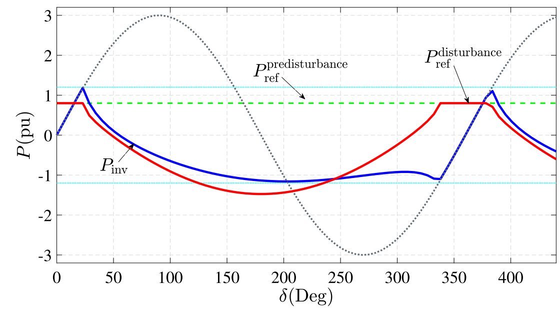

FIGURE 12. Power angle relationship for a GFM-IBR with a circular current limiter and the proposed solution.

Fig. 11 illustrates the minimum value of k for different SCRs of the grid. As illustrated in Fig. 11, larger k values are required for larger SCRs of the grid. Therefore, the k value must be selected based on the SCRs for all the possible configurations of the grid. Fig. 12 illustrates the new power angle curve of the inverter after considering P_{add}.

It is worth noting that voltage-based methods have been previously proposed in the literature to improve critical clearing time during voltage drops caused by disturbances [32]. The existing methods in the literature reduce the active reference power based on voltage at the terminal of the inverter as given in (12)-(14).

$$S_{new} = V_{opu} S_{nom} \tag{12}$$

$$Q_{ref}^{new} = \begin{cases} Q_{ref} & \text{if } V_{opu} \geq 0.9 \\ 2S_{new}(1 - V_{opu}) & \text{if } 0.5 \leq V_{opu} < 0.9 \\ S_{new} & \text{otherwise} \end{cases} \tag{13}$$

$$P_{ref}^{new} = \sqrt{S_{new}^2 - Q_{ref}^{new}} \tag{14}$$

where S_{nom} denotes the nominal power of the inverter in normal conditions and V_{opu} denotes the output voltage of the inverter at the point of common coupling in per-unit. This method is unable to address pole slipping caused by voltage phase angle jumps. A comparative study is provided in the simulation results section to highlight the differences between the proposed method and the existing voltage-based methods in the literature.

TABLE 2. Values of the parameters used in simulation and experimental tests.

Parameter	Unit	Simulation	Experiment
Nominal Power	(kVA)	35	1
Nominal Voltage	(V)	400	125
ω_b	(rad/sec)	$2\pi60$	$2\pi60$
L_f, R_f , C_f	(pu)	0.13, 0.0028, 0.06	0.12, 0.0004, 0.0
$f_{\text{switching}}$	(kHz)	10	20
t_{sampling}	(μs)	1	50
P_{ref},Q_{ref}	(pu)	0.8, 0	0.8, 0
m_p, m_q	(pu)	0.02, 0.1	0.02, 0.1
ω_{pcf},ω_{qcf}	(pu)	0.1, 0.1	0.1, 0.1
ω_0	(pu)	1	1
V_{ref}	(pu)	1	1
k_{pv}, k_{iv}	(A/V), (A/V.s)	1.9, 4.26	0.15, 0.00134
k_{pi}, k_{ii}	(V/A), (V/A.s)	6.34π, 52π	5, 6.75

V. TIME DOMAIN SIMULATION

This section provides time-domain simulation results for pole slipping in GFM-IBRs. The validity and correctness of the proposed solution for preventing pole slipping is further tested and verified. Test system shown in Fig. 3 is used to implement simulations. The detailed parameters of the system under study are provided in Table 2. Time-domain simulations are conducted using MATLAB Simulink.

A. DYNAMIC RESPONSE OF GFM-IBRS TO VOLTAGE PHASE ANGLE JUMP

Simulation results for the dynamic response of GFM-IBRs to voltage phase angle jump without voltage drop are provided in this subsection. Three scenarios can occur, as discussed in Section II-B, depending on the disturbance severity, the operating point of the IBR, and grid conditions. In the figures of Section V-A, (a), (b), (c), and (d) denote power angle, current magnitude, power output, and voltage magnitude at PCC, respectively. It is worth noting that the voltage phase angle is compared with the power angle in each scenario to distinguish their behavior across various conditions.

1) SCENARIO 1 – RESTORATION TO A STABLE OPERATING POINT WITHOUT POLE SLIPPING

In scenario 1, a voltage phase angle jump equal to $-10°$ is considered to appear at the upstream bus of the GFM-IBR. The active power output and the reference active power of the IBR before the disturbance are considered to be equal to 0.8 pu. Moreover, the SCR of the grid is considered to be equal to 3.6. A phase jump equal to $-10°$ happens at $t = 0$ s. The current limiting mechanism activates, and as illustrated in Fig. 13, the inverter current increases to 1.2 pu upon the current limiter activation. The active power output of the inverter further increases and becomes larger than the reference power, which remains constant during the disturbance. As a result, the power angle decreases from 13° to 3° without pole slipping. Although the current limit is activated, the phase change is not large enough to pass critical voltage phase angle jump according to Fig. 5. Therefore, the inverter power angle returns to a stable equilibrium point.

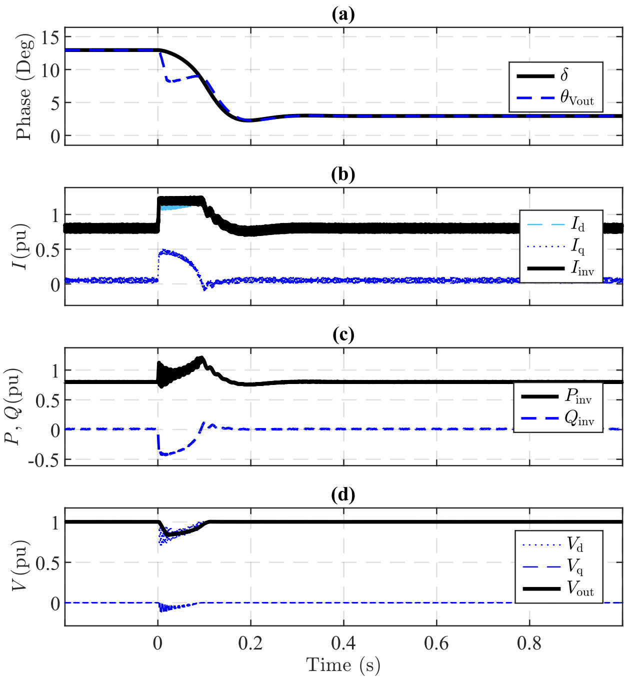

FIGURE 13. GFM-IBR response in Scenario 1 (restoration to stable operating point): SCR=3.6, $P_{\text{ref}} = 0.8$ pu, and phase jump=$-10°$.

2) SCENARIO 2 – STABLE POLE SLIPPING

In scenario 2, voltage phase angle jump equal to $-20°$ is considered to appear at the upstream bus of the GFM-IBR at $t = 0$ s. The reference active power of the IBR, and SCR of the grid are considered to be similar to scenario 1. Fig. 14 demonstrates the dynamic response of the IBR. As illustrated in the figure, the inverter current increases to 1.2 pu, similar to scenario 1. However, the active power output of the inverter decreases in this case in contrast to scenario 1. As a result, the power angle increases from 13° to 353°, instead of decreasing to $-7°$, and pole slipping occurs.

3) SCENARIO 3 – UNSTABLE POLE SLIPPING

In this scenario, a voltage phase angle jump equal to $-10°$, similar to the first scenario, is considered to appear at the upstream bus of the GFM-IBR. In this scenario, the pre-disturbance active power output and the reference active power of the IBR are considered to be equal to 0.85 pu. Moreover, the SCR of the grid has increased to 6.5. Fig. 15 demonstrates the dynamic response of the IBR. As a result of the disturbance, the inverter current increases to 1.2 pu, similar to scenarios 1 and 2. The active power output of the inverter decreases in this case similar to scenario 2. However, the power angle continually increases and unstable pole slipping occurs. This test shows how a small phase jump leads to instability in high SCRs.

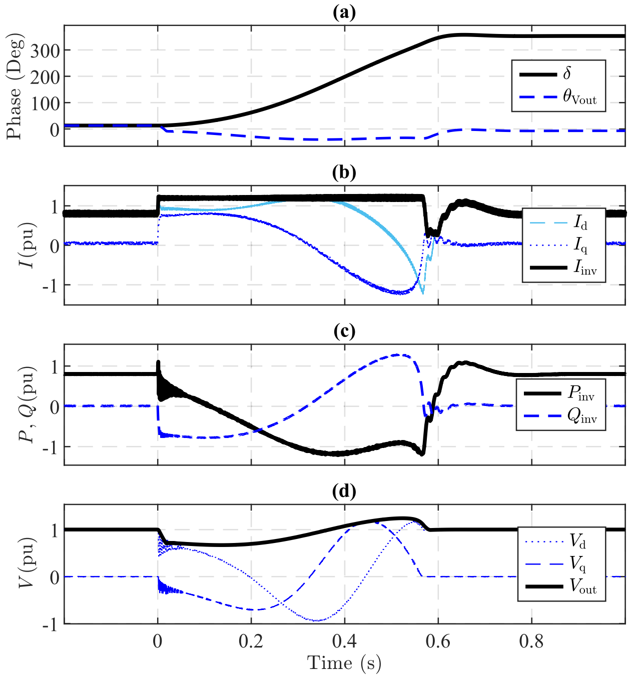

FIGURE 14. GFM-IBR response in Scenario 2 (stable pole slipping): SCR=3.6, P_{ref} = 0.8 pu, and phase jump=−20°.

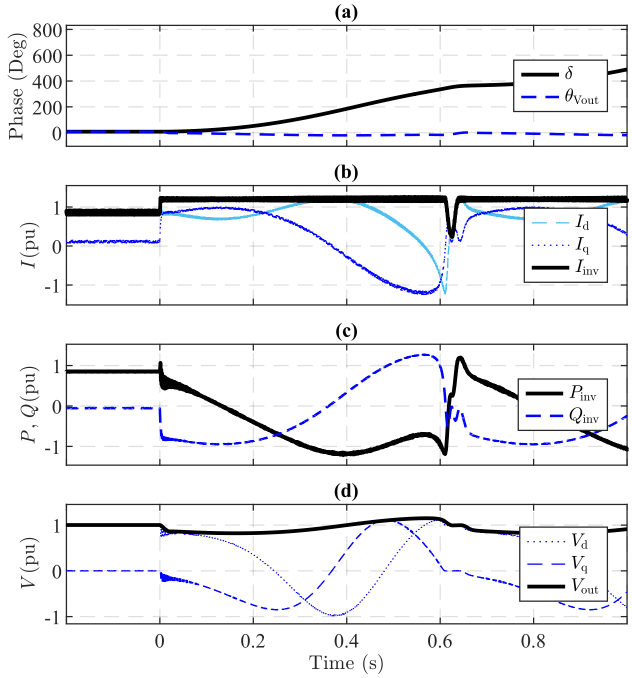

FIGURE 15. GFM-IBR response in Scenario 3 (unstable pole slipping): SCR=6.5, P_{ref}=0.85 pu, and phase jump=−10°.

B. PROPOSED METHOD PERFORMANCE EVALUATION

The performance of the proposed solution is presented through EMT simulations. The method was evaluated with respect to a conventional circular current limiter and an existing voltage-based method mentioned in the previous section. Due to the space limit, only voltages, currents, and powers are shown in the following simulations. For current and voltage, d-q components are also included in the figures for more clarification.

1) VOLTAGE DROP WITHOUT VOLTAGE PHASE ANGLE JUMP

Severe voltage drops without phase angle jump can also cause pole slipping in GFM-IBRs. In the first simulation, the inverter initially operates at P_{ref}=0.8 pu in SCR=6. A voltage drop equal to 0.9 pu is considered on the upstream bus of the GFM-IBR at $t = 0$ s. During the fault, the inverter voltage drops and the current limiter is activated. After 0.2 s, the fault is cleared, and the grid voltage rises. However, as discussed in Section II, the phase angle jump is more than the critical value, and the inverter passes the next equilibrium point. Therefore, the inverter current remains saturated. As a result of the severe voltage drop, the inverter experiences a pole slipping during the postfault stage, as shown in Fig. 16. The figure demonstrates the dynamic response of the inverter, including the conventional circular current limiter. Figs. 17 and 18 illustrate that the existing voltage-based method and the proposed solution can both prevent pole slipping caused by severe voltage drops in approximately high SCRs.

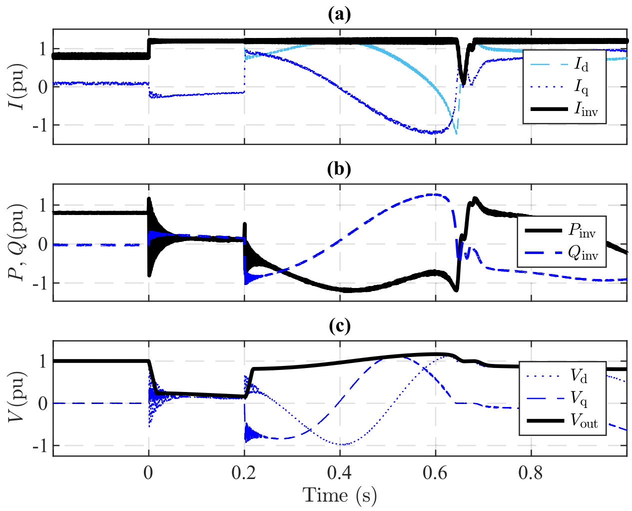

FIGURE 16. The response of GFM-IBR with the conventional circular current limiter to a 0.9 pu voltage drop without phase angle jump in a stiff grid: (a) current magnitude, (b) power output, (c) voltage magnitude at PCC.

2) STABLE POLE SLIPPING CAUSED BY VOLTAGE PHASE ANGLE JUMP

This case study demonstrates that voltage phase angle jump can also cause stable pole slipping in GFM-IBRs. Fig. 19 demonstrates the dynamic response of the inverter without implementing the voltage-based method or the proposed solution. As illustrated in Fig. 20, the voltage-based method is unable to prevent pole slipping when there is a voltage phase angle jump without voltage drop. In contrast, the proposed

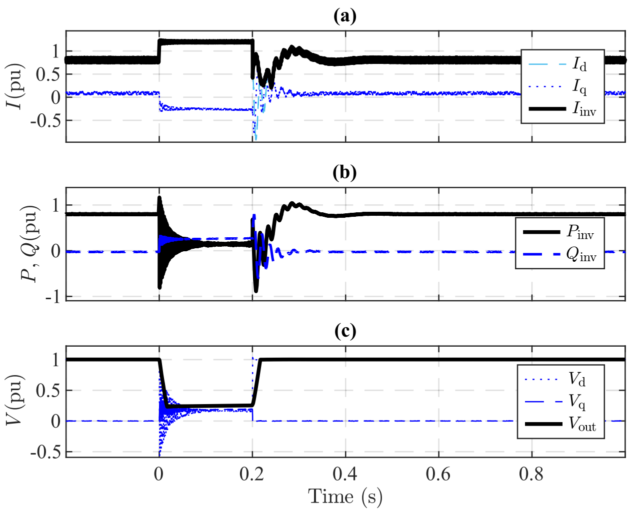

FIGURE 17. **The response of GFM-IBR with the voltage-based method to a 0.9 pu voltage drop without phase angle jump in a stiff grid: (a) current magnitude, (b) power output, (c) voltage magnitude at PCC.**

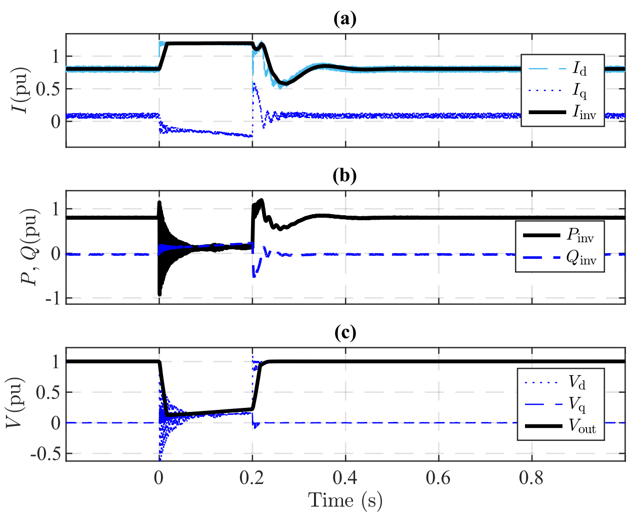

FIGURE 18. **The response of GFM-IBR with the proposed method to a 0.9 pu voltage drop without phase angle jump in a stiff grid: (a) current magnitude, (b) power output, (c) voltage magnitude at PCC.**

solution, shown in Fig. 21, can prevent pole slipping even for cases with severe voltage phase angle jump, i.e., 60°. It is worth noting that the proposed solution prevents the overvoltage problem caused by pole slipping and reduces the reverse power problem.

3) UNSTABLE POLE SLIPPING CAUSED BY VOLTAGE PHASE ANGLE JUMP

In this case, a severe voltage phase angle jump equal to $-60°$ occurs at $t = 0$ s while SCR=6 and $P_{\text{ref}} = 0.8$ pu. Initially, the inverter operates in normal conditions. Upon the occurrence of the disturbance, the inverter current limiter is activated due to the severity of the disturbance. The conventional circular current limiter, as expected, undergoes an unstable pole slipping, as shown in Fig. 22. As can be seen in Fig. 23, the voltage-based method is also unable to prevent unstable pole

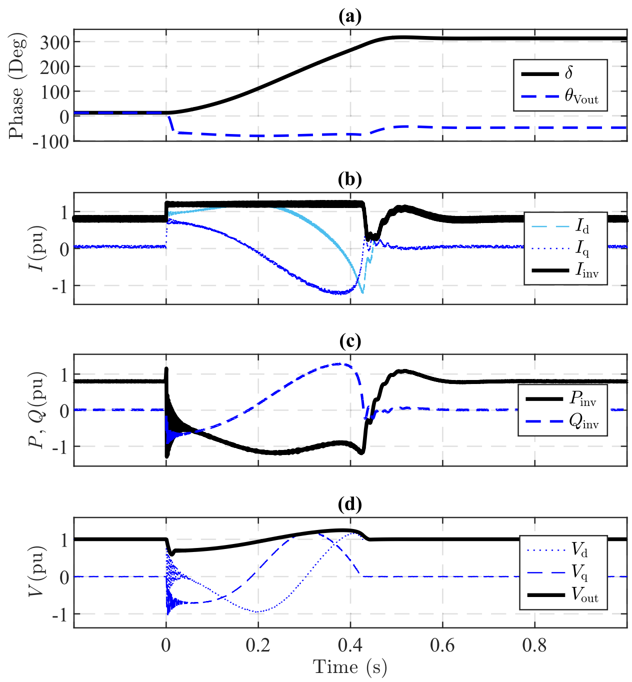

FIGURE 19. **The response of GFM-IBR with the conventional circular current limiter to a voltage phase angle jump=−60° when SCR=3.5: (a) power angle, (b) current magnitude, (c) power output, (d) voltage magnitude at PCC.**

slipping when there is a voltage phase angle jump without voltage drop. The proposed solution, however, can prevent unstable pole slipping and restore the inverter to its new normal operating point in less than 0.6 s, shown in Fig. 24. As such, the advantage of the proposed method compared with the existing voltage-based methods is significant.

VI. EXPERIMENTAL RESULTS

This section experimentally investigates the dynamic response of GFM-IBRs under varying voltage phase angle disturbances and different grid strengths. It also validates the effectiveness of the proposed mitigation method. The experimental setup includes an Imperix Power Rack, with controllers developed and deployed on an Imperix B-Box platform. The inverter connects to a Regatron TC.ACS grid simulator via LC filters and emulated grid impedance. Fig. 25 shows the experimental setup of the system under the study. Table 2 provides detailed parameters of the experimental setup.

A. DYNAMIC RESPONSE OF GFM-IBRS TO VOLTAGE PHASE ANGLE JUMPS

Voltage phase angle jumps are common disturbances in power systems, particularly in weak grid conditions. This subsection examines the GFM-IBR's response to such disturbances with a SCR of 2 and an initial active power reference (P_{ref}) of 0.8 pu. The analysis considers both small and large voltage phase angle jumps, with and without the proposed mitigation method.

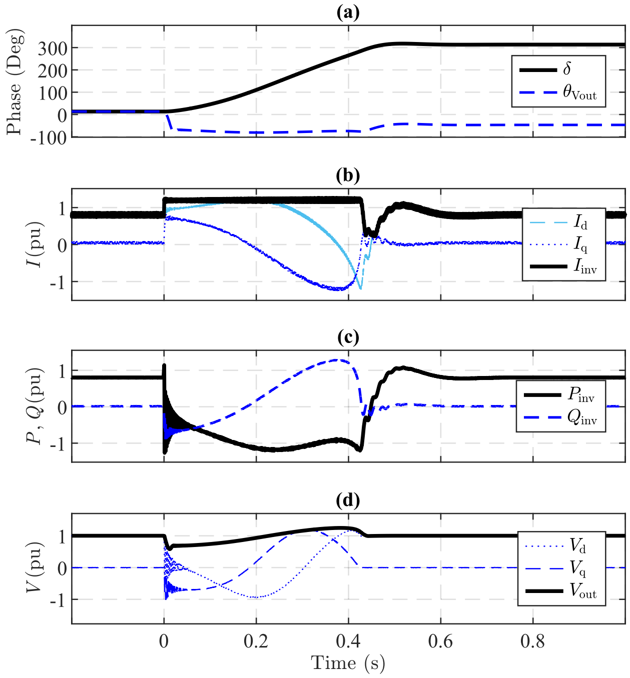

FIGURE 20. The response of GFM-IBR with the voltage-based method to a voltage phase angle jump=−60° when SCR=3.5: (a) power angle, (b) current magnitude, (c) power output, (d) voltage magnitude at PCC.

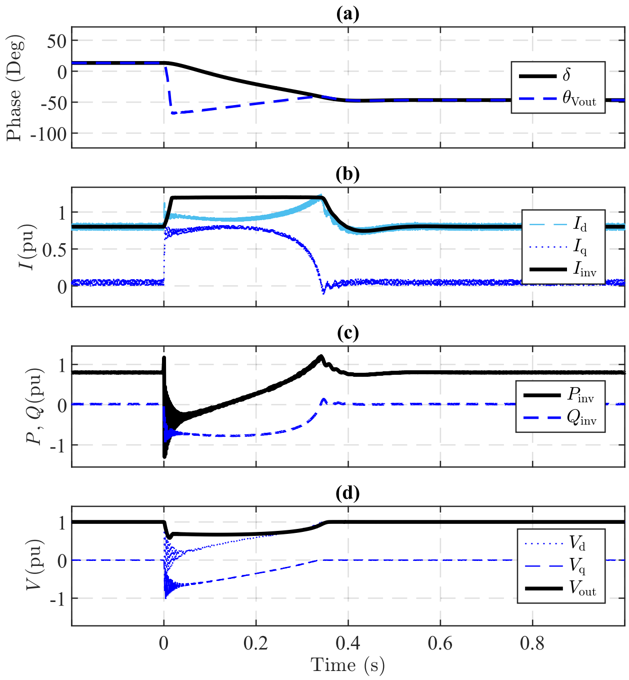

FIGURE 21. The response of GFM-IBR with the proposed method to a voltage phase angle jump=−60° when SCR=3.5: (a) power angle, (b) current magnitude, (c) power output, (d) voltage magnitude at PCC.

1) CASE 1: VOLTAGE PHASE ANGLE JUMP OF −10°

When a $-10°$ phase angle jump occurs, the current limiting mechanism of the GFM-IBR activates and caps the inverter current at 1.2 pu. As shown in Fig. 26, the active power output temporarily exceeds the reference power, resulting in a reduction in the power angle. The inverter stabilizes without experiencing pole slipping, demonstrating that small disturbances can be mitigated by the inverter's inherent dynamics in weak grid conditions.

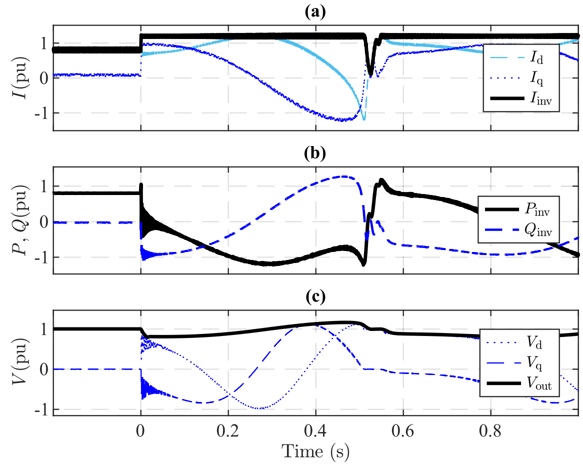

FIGURE 22. The response of GFM-IBR with the conventional circular current limiter to a severe voltage phase angle jump when SCR=6: (a) current magnitude, (b) power output, (c) voltage magnitude at PCC.

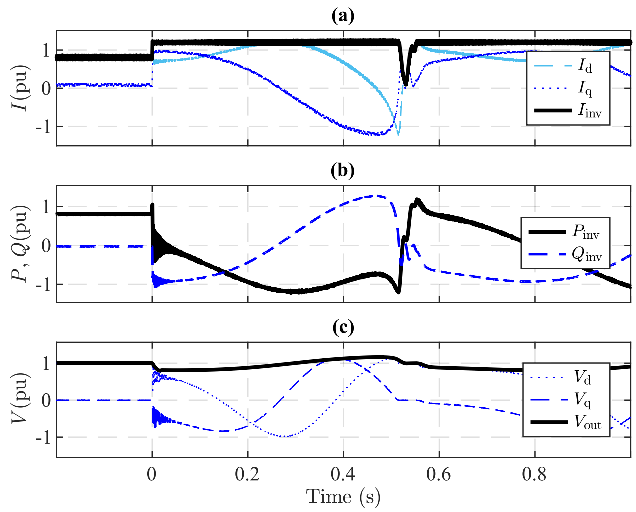

FIGURE 23. The response of GFM-IBR with the voltage-based method to a severe voltage phase angle jump when SCR=6: (a) current magnitude, (b) power output, (c) voltage magnitude at PCC.

2) CASE 2: VOLTAGE PHASE ANGLE JUMP OF −20°

When the phase angle jump increases to $-20°$, the current limiters activate again, but the inverter exhibits stable pole slipping, as shown in Fig. 27. The power angle shifts significantly beyond 180°, causing the inverter to momentarily lose synchronism with the grid.

With the proposed mitigation method, the GFM-IBR dynamically adjusts its active power reference during the disturbance, allowing the inverter to stabilize at a new equilibrium point. Fig. 28 demonstrates that the proposed method effectively prevents stable pole slipping under the $-20°$ disturbance. By addressing the power mismatch,

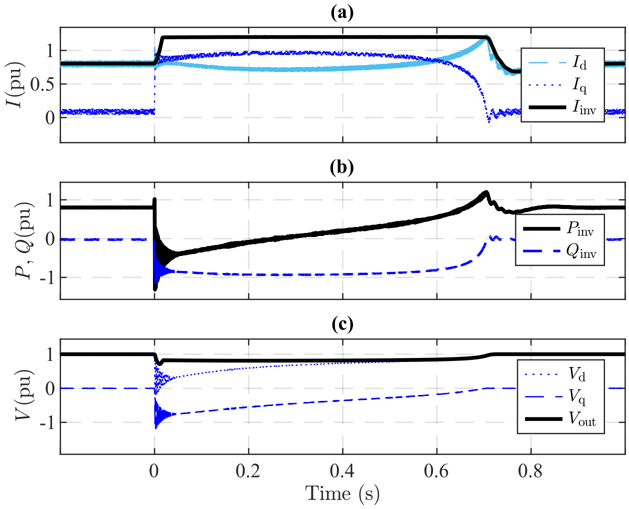

FIGURE 24. The response of GFM-IBR with the proposed method to a severe voltage phase angle jump when SCR=6: (a) current magnitude, (b) power output, (c) voltage magnitude at PCC.

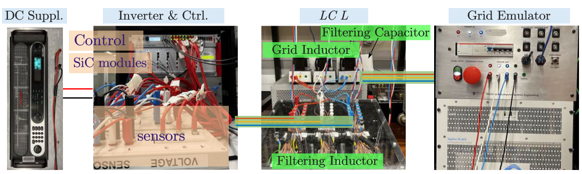

FIGURE 25. Experimental setup of the system under the study; the inverter is connected to a DC supply(left) and LCL filter is included to connect the inverter to the Grid (Right Emulator).

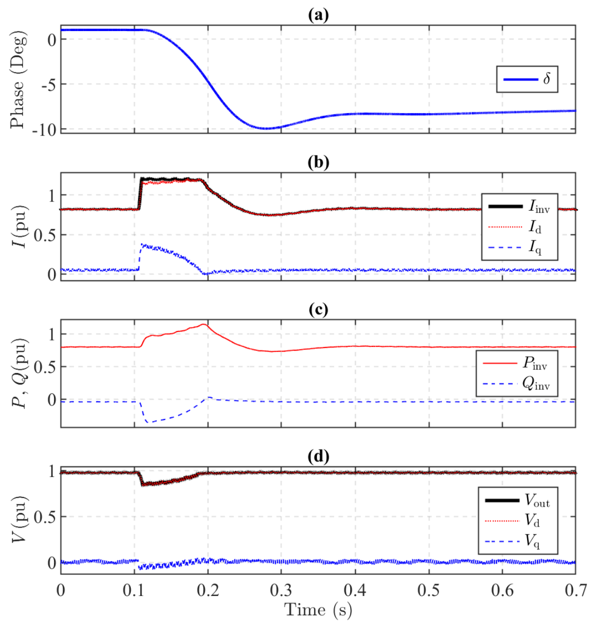

FIGURE 26. Experimental results of the GFM-IBR with the conventional circular current limiter: voltage phase angle jump=−10° at SCR=2 with no pole slip observed: (a) Power angle, (b) d-q components of the grid current and magnitude, (c) Active and reactive power at the PCC, (d) d-q components of the voltage and magnitude at the PCC.

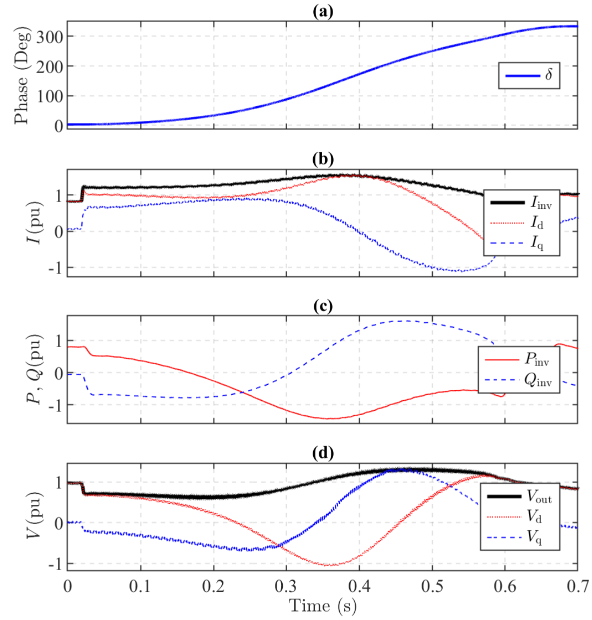

FIGURE 27. Experimental results of the GFM-IBR with the conventional circular current limiter: voltage phase angle jump=−20° at SCR=2 with stable pole slip observed: (a) Power angle, (b) d-q components of the grid current and magnitude, (c) Active and reactive power at the PCC, (d) d-q components of the voltage and magnitude at the PCC.

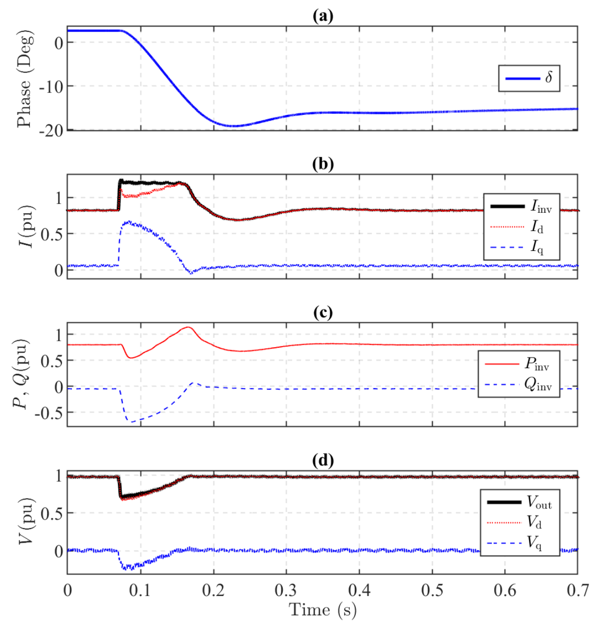

FIGURE 28. Experimental results of the GFM-IBR with the proposed method: voltage phase angle jump=−20° at SCR=2 with no pole slip observed: (a) power angle, (b) d-q components of the grid current and magnitude, (c) active and reactive power at the PCC, (d) and d-q components of the voltage and magnitude at the PCC.

the method ensures that the system remains synchronized even in weak grid conditions.

B. UNSTABLE POLE SLIPPING AND PERFORMANCE OF THE PROPOSED METHOD

Unstable pole slipping, characterized by continuous oscillations of the power angle beyond 180°, represents a severe stability issue for GFM-IBRs. This subsection examines the

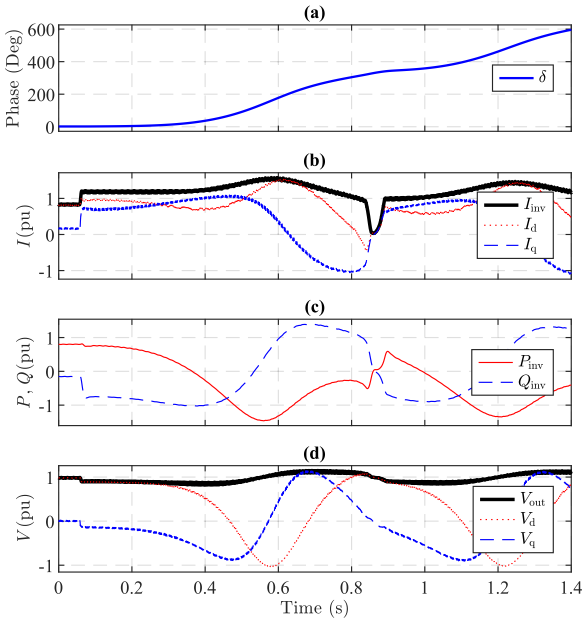

FIGURE 29. Experimental results of the GFM-IBR with the conventional circular current limiter: voltage phase angle jump = $-10°$ at SCR=10 with unstable pole slip observed: (a) power angle, (b) d-q components of the grid current and magnitude, (c) active and reactive power at the PCC, and (d) d-q components of the voltage and magnitude at the PCC.

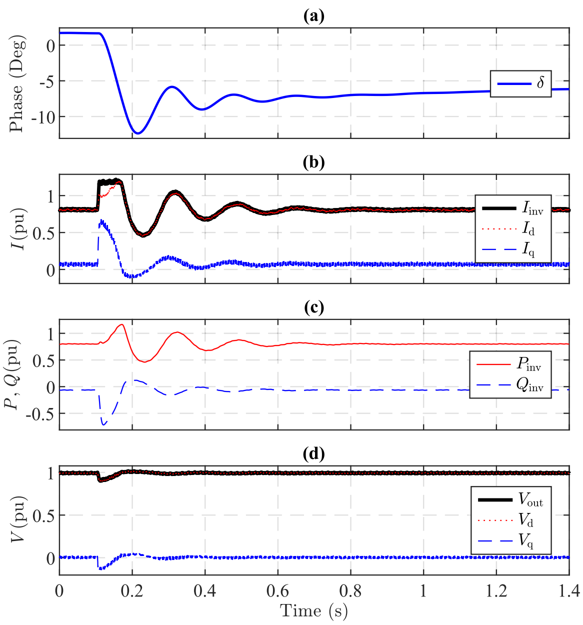

FIGURE 30. Experimental results of the GFM-IBR with the proposed method: voltage phase angle jump = $-10°$ at SCR=10 with no pole slip observed: (a) power angle, (b) d-q components of the grid current and magnitude, (c) active and reactive power at the PCC, and (d) d-q components of the voltage and magnitude at the PCC.

inverter's response to a $-10°$ voltage phase angle jump under strong grid conditions, with SCR set to 10 and $P_{\text{ref}} = 0.8$ pu.

1) CONVENTIONAL CIRCULAR CURRENT LIMITER

Fig. 29 illustrates the inverter's response with the conventional circular current limiter. The current limiting mechanism activates, but the system fails to stabilize. The power angle oscillates continuously, and the inverter loses synchronism with the grid. This result highlights the inability of conventional current limiters to address unstable pole slipping in strong grid conditions, where disturbances can induce instability.

2) PROPOSED METHOD

When the proposed mitigation method is applied, the inverter dynamically adjusts its active power reference to manage the disturbance. Fig. 30 shows that the system successfully stabilizes at a new operating point, effectively mitigating unstable pole slipping. The proposed method ensures that the power angle remains within stable bounds, enabling the inverter to maintain synchronism even in the presence of significant phase angle disturbances.

VII. CONCLUSION

This paper described the notion of pole slipping in droop-based grid forming inverters with circular current limiters. It is demonstrated that both voltage drop and voltage phase angle jump can cause pole slipping in grid forming inverters. It is shown that the strength of the grid and the operating point of the inverter before the disturbance are determining factors for the occurrence of pole slipping in grid forming inverters. The analysis shows that unstable pole slipping might occur in SCRs greater than 3.5 It is further demonstrated that pole slipping creates overvoltage. The results revealed the overvoltage can exceed 1.2 pu in SCRs lower than 4.85. Other challenges associated with pole slipping is reverse active power flow and overloading for grid forming inverters. The conditions for stable and unstable pole slipping are further derived and discussed in detail. It is found that increasing the droop gain and decreasing cut-off frequency of the low-pass filter in the droop loop increase the chance of pole slipping. A control strategy is proposed to prevent pole slipping in grid forming inverters. The advantages of the proposed strategy is demonstrated in comparison with an existing voltage-based strategy in grid forming inverters during voltage drops. The theoretical analysis and simulation results are validated by experimental analysis. In our future research work the impact of pole slipping in GFM-IBRs on swing and out-of-step protection will be investigated. Moreover, the system-wide implications of pole slipping in GFM-IBRs on large multi-machine systems will be examined.

APPENDIX

The active power output of droop-based GFM-IBRs with a circular current limiter is derived here based on [19]. A grid forming voltage source converter with a circular current limiter is illustrated in Fig. 3. The voltage source converter is connected to the rest of the grid through an LC filter with the resistance r_f, inductance l_f, and capacitance c_f. The resistance and inductance of the grid are denoted by r_g and l_g, respectively. The $P-f$ droop control given in (15) is applied to synchronize the converter with the grid.

$$\omega = m_p \frac{\omega_{\text{pcf}}}{s + \omega_{\text{pcf}}} (P_{\text{ref}} - P_{\text{inv}}) + \omega_0 \tag{15}$$

The circular current limiter in the dq frame is further employed to protect the converter as given in (16).

$$i_{\text{dq,ref}} = K_{\text{lim}} i_{\text{cdq,ref}}, \quad K_{\text{lim}} = \min\{1, \frac{I_{\text{th}}}{||i_{\text{cdq,ref}}||}\} \tag{16}$$

where $i_{\text{dq,ref}}$ and $i_{\text{cdq,ref}}$ denote the output of the circular current limiter and current generated by the voltage controller, respectively. K_{lim} denotes the ratio of the output and input of the circular current limiter. In the normal operating conditions K_{lim} is equal to 1 and K_{lim} is less than 1 when the circular current limiter is activated.

We adopt the equivalent circuit model of the grid forming voltage source converters with the circular current limiters from [19]. As described in [19], the circular current limiter becomes activated after the occurrence of a disturbance, and the voltage integral controller is changed to zero to prevent wind-up. Thus, the grid forming voltage source converter can be modelled as a voltage source behind a resistance as given in (17). It is worth noting that the current control loop dynamics is ignored in the derivation of (17) [19].

$$v_{dq} = v_{\text{dq,ref}} - r_e i_{\text{dq}} \tag{17}$$

where v_{dq} and $v_{dq,\text{ref}}$ denote the voltage of the point of common coupling and the reference voltage for the point of common coupling, respectively. r_e is a real and non-negative variable which is given by (18).

$$r_e = \frac{1 - K_{\text{lim}}}{K_{\text{lim}} k_{\text{pv}}} \tag{18}$$

where k_{pv} is the proportional gain of the voltage controller block. It is worth noting r_e is equal to zero during normal operating conditions.

As described in [19], the active power of the inverter can be derived using the Kirchhoff circuit law and (17) as given in Section II-B. It is worth noting that the changes in the voltage phase angle in the upstream bus and the droop low-pass filter are ignored in [19] which are considered in this paper.

ACKNOWLEDGMENT

The authors would like to express their sincere appreciation to Dr. Seyed Fariborz Zarei from Qom University of Technology for the valuable advice and insightful comments during the revision of this paper.

REFERENCES

[1] A. Sajadi, J. A. Rañola, R. W. Kenyon, B.-M. Hodge, and B. Mather, "Dynamics and stability of power systems with high shares of grid-following inverter-based resources: A tutorial," *IEEE Access*, vol. 11, pp. 29591–29613, 2023.

[2] R. Luo, H. Gao, F. Peng, and Y. Guo, "An adaptive low-voltage ride-through method for virtual synchronous generators during asymmetrical grid faults," *IEEE Trans. Sustain. Energy*, vol. 15, no. 3, pp. 1589–1600, Jul. 2024.

[3] J. D. Fernández, J. Eloy-García, E. R. Navarro, S. A. Gómez, and J. L. R. Amenedo, "Low-voltage ride-through algorithm for grid-forming converters," *IEEE Trans. Power Electron.*, vol. 40, no. 1, pp. 303–315, Jan. 2025.

[4] L. Huang and F. Blaabjerg, "A reference frame rematching method for enhancing large-signal stability of grid-following inverter under weak grid," *IEEE Trans. Power Electron.*, vol. 40, no. 4, pp. 6135–6146, Apr. 2025.

[5] M. F. M. Arani and Y. A. I. Mohamed, "Analysis and performance enhancement of vector-controlled VSC in HVDC links connected to very weak grids," *IEEE Trans. Power Syst.*, vol. 32, no. 1, pp. 684–693, Jan. 2017.

[6] X. Wang, M. G. Taul, H. Wu, Y. Liao, F. Blaabjerg, and L. Harnefors, "Grid-synchronization stability of converter-based resources—An overview," *IEEE Open J. Ind. Appl.*, vol. 1, pp. 115–134, 2020.

[7] F. Blaabjerg, Y. Yang, D. Yang, and X. Wang, "Distributed power-generation systems and protection," *Proc. IEEE*, vol. 105, no. 7, pp. 1311–1331, Jul. 2017.

[8] B. Bahrani, M. H. Ravanji, B. Kroposki, D. Ramasubramanian, X. Guillaud, T. Prevost, and N.-A. Cutululis, "Grid-forming inverter-based resource research landscape: Understanding the key assets for renewable-rich power systems," *IEEE Power Energy Mag.*, vol. 22, no. 2, pp. 18–29, Mar. 2024.

[9] C. Fang, L. Mu, Z. Wang, and G. Chen, "Analysis of grid-forming IIDG's transient- and steady-state fault model," *IEEE Trans. Smart Grid*, vol. 13, no. 2, pp. 1187–1199, Mar. 2022.

[10] B. Fan and X. Wang, "Fault recovery analysis of grid-forming inverters with priority-based current limiters," *IEEE Trans. Power Syst.*, vol. 38, no. 6, pp. 5102–5112, Nov. 2023

[11] K. G. Saffar, S. Driss, and F. B. Ajaei, "Impacts of current limiting on the transient stability of the virtual synchronous generator," *IEEE Trans. Power Electron.*, vol. 38, no. 2, pp. 1509–1521, Feb. 2023.

[12] D. Li, Q. Sun, R. Wang, and Z. Sui, "Transient stability analysis and enhancement of inverter-based microgrid considering current limitation," *IEEE Trans. Power Electron.*, vol. 40, no. 1, pp. 2429–2441, Jan. 2025.

[13] J. Chen, F. Prystupczuk, and T. O'Donnell, "Use of voltage limits for current limitations in grid-forming converters," *CSEE J. Power Energy Syst.*, vol. 6, no. 2, pp. 259–269, Jun. 2020.

[14] E. Rokrok, T. Qoria, A. Bruyere, B. Francois, and X. Guillaud, "Transient stability assessment and enhancement of grid-forming converters embedding current reference saturation as current limiting strategy," *IEEE Trans. Power Syst.*, vol. 37, no. 2, pp. 1519–1531, Mar. 2022.

[15] Z. Li, K. W. Chan, J. Hu, and S. W. Or, "An adaptive fault ride-through scheme for grid-forming inverters under asymmetrical grid faults," *IEEE Trans. Ind. Electron.*, vol. 69, no. 12, pp. 12912–12923, Dec. 2022.

[16] B. Mahamedi, M. Eskandari, J. E. Fletcher, and J. Zhu, "Sequence-based control strategy with current limiting for the fault ride-through of inverter-interfaced distributed generators," *IEEE Trans. Sustain. Energy*, vol. 11, no. 1, pp. 165–174, Jan. 2020.

[17] M. Eskandari and A. V. Savkin, "On the impact of fault ride-through on transient stability of autonomous microgrids: Nonlinear analysis and solution," *IEEE Trans. Smart Grid*, vol. 12, no. 2, pp. 999–1010, Mar. 2021.

[18] L. Huang, H. Xin, Z. Wang, L. Zhang, K. Wu, and J. Hu, "Transient stability analysis and control design of droop-controlled voltage source converters considering current limitation," *IEEE Trans. Smart Grid*, vol. 10, no. 1, pp. 578–591, Jan. 2019.

[19] B. Fan and X. Wang, "Equivalent circuit model of grid-forming converters with circular current limiter for transient stability analysis," *IEEE Trans. Power Syst.*, vol. 37, no. 4, pp. 3141–3144, Jul. 2022.

[20] N. Karimipour, M. F. M. Arani, and A. Abiri Jahromi, "Investigating disturbance-induced misoperation of grid-following inverter-based resources," *IET Gener., Transmiss. Distrib.*, vol. 19, no. 1, Jan. 2025, Art. no. e70046.

[21] L. Fan, Z. Wang, and Z. Miao, "Large angle deviation in grid-following IBRs upon grid voltage dip," *IEEE Trans. Energy Convers.*, vol. 39, no. 1, pp. 368–378, Mar. 2024.

[22] R. Bauer, H. Gugel, M. Lauby, M. Lewis, D. Moore, J. Moura, R. Quint, A. Shattuck, A. Thant, D. Penney, F. Garcia, P. Gravois, J, Hariharan, S.-H. Huang, J. Schmall, S. Solis, and S. W. Kang, "Odessa disturbance Texas event: June 4, 2022 joint nerc and Texas RE staff report," Joint NERC and Texas RE Staff Report, Atlanta, GA, USA, Tech. Rep., Dec. 2022.

[23] M. A. Redfern and M. J. Checksfield, "A review of pole slipping protection," in *Proc. IEE Colloq. Generator Protection*, Newcastle upon Tyne, U.K., 1996, pp. 6/1–6/9, doi: 10.1049/ic:19961407.

[24] M. Abdi-Khorsand and V. Vittal, "Modeling protection systems in time-domain simulations: A new method to detect MIS-operating relays for unstable power swings," *IEEE Trans. Power Syst.*, vol. 32, no. 4, pp. 2790–2798, Jul. 2017.

[25] P. Kundur, "Power system stability," in *Power System Stability and Control*. New York, NY, USA: McGraw-Hill, Inc., 2007, pp. 1–7.

[26] M. A. Redfern and M. J. Checkfield, "A new pole slipping protection algorithm for dispersed storage and generation using the equal area criterion," *IEEE Trans. Power Del.*, vol. 10, no. 1, pp. 194–202, Jan. 1995.

[27] E. Farantatos, R. Huang, G. J. Cokkinides, and A. P. Meliopoulos, "A predictive generator out-of-step protection and transient stability monitoring scheme enabled by a distributed dynamic state estimator," *IEEE Trans. Power Del.*, vol. 31, no. 4, pp. 1826–1835, Aug. 2016.

[28] M. A. Redfern and M. J. Checksfield, "A study into a new solution for the problems experienced with pole slipping protection [of synchronous generators]," *IEEE Trans. Power Del.*, vol. 13, no. 2, pp. 394–404, Apr. 1998.

[29] H. Ashrafi, S. Brahma, D. Finney, N. Fischer, D. Fredrickson, J. Gers, R. Gokaraju, G. Henneberg, P. Kumar, and M. Nagpal, "Application of out-of-step protection schemes for generators," Power Syst. Relaying Control Committee (PSRC), Denver, CO, USA, Tech. Rep. PES-TR79, 2020.

[30] M. G. Taul, X. Wang, P. Davari, and F. Blaabjerg, "Current limiting control with enhanced dynamics of grid-forming converters during fault conditions," *IEEE J. Emerg. Sel. Topics Power Electron.*, vol. 8, no. 2, pp. 1062–1073, Jun. 2020.

[31] S. F. Zarei, H. Mokhtari, M. A. Ghasemi, and F. Blaabjerg, "Reinforcing fault ride through capability of grid forming voltage source converters using an enhanced voltage control scheme," *IEEE Trans. Power Del.*, vol. 34, no. 5, pp. 1827–1842, Oct. 2019.

[32] S. P. Me, S. Zabihi, F. Blaabjerg, and B. Bahrani, "Adaptive virtual resistance for postfault oscillation damping in grid-forming inverters," *IEEE Trans. Power Electron.*, vol. 37, no. 4, pp. 3813–3824, Apr. 2022.

[33] T. Qoria, F. Gruson, F. Colas, G. Denis, T. Prevost, and X. Guillaud, "Critical clearing time determination and enhancement of grid-forming converters embedding virtual impedance as current limitation algorithm," *IEEE J. Emerg. Sel. Topics Power Electron.*, vol. 8, no. 2, pp. 1050–1061, Jun. 2020.

[34] *IEEE Standard for Interconnection and Interoperability of Inverter-Based Resources (IBRS) Interconnecting With Associated Transmission Electric Power Systems*, Standard 2800-2022, 2022.

[35] *IEEE Standard for Interconnection and Interoperability of Distributed Energy Resources With Associated Electric Power Systems Interfaces—Amendment 1: To Provide More Flexibility for Adoption of Abnormal Operating Performance Category III*, Standard 1547a-2020 (Amendment to IEEE Std 1547-2018), 2020.

NEGAR KARIMIPOUR (Member, IEEE) received the B.Sc. degree in electrical engineering-power from Isfahan University of Technology, Isfahan, Iran, in 2012, and the M.Sc. degree in electrical engineering-power electronics from Tarbiat Modares University, Tehran, Iran, in 2014. She is currently pursuing the Ph.D. degree with the Department of Electrical, Computer, and Biomedical Engineering, Toronto Metropolitan University, Toronto, ON, Canada. Her research interests include modeling and control of power electronics systems, grid integration of renewable energy resources, power system dynamics, and stability analysis.

HANSI WIJAYALATH ARACHCHILAGE (Graduate Student Member, IEEE) received the B.Sc. degree in electrical engineering from the University of Moratuwa, Moratuwa, Sri Lanka, in 2022. She is currently pursuing the Ph.D. degree in electrical engineering with Monash University, Clayton, VIC, Australia. As part of the Ph.D. studies, she contributed to the development of Australia's Global Power System Transformation Research Roadmap, led by CSIRO in partnership with the Global Power System Transformation Consortium. Her research interests include the control and transient stability analysis of grid-following and grid-forming inverter-based resources, as well as the integration of renewable energy sources into power systems.

AMIR ABIRI JAHROMI (Senior Member, IEEE) received the Ph.D. degree in electrical and computer engineering from McGill University, Montréal, QC, Canada, in 2016. From January 2018 to December 2019, he was a Postdoctoral Fellow with the University of Toronto, Toronto, ON, Canada, where he was a Research Associate in 2020. He is currently a Lecturer with the School of Electronic and Electrical Engineering, University of Leeds, Leeds, U.K. His research interests include power system modeling, cyber–physical security, reliability, economics, and optimization of power systems.

BEHROOZ BAHRANI (Senior Member, IEEE) received the B.Sc. degree from Sharif University of Technology, Tehran, Iran, the M.Sc. degree from the University of Toronto, Toronto, ON, Canada, and the Ph.D. degree from the École Polytechnique Fédérale de Lausanne (EPFL), Lausanne, Switzerland, all in electrical engineering, in 2006, 2008, and 2012, respectively. From September 2012 to September 2015, he was a Postdoctoral Fellow at several institutions, including EPFL, Purdue University, West Lafayette, IN, USA, Georgia Institute of Technology, Atlanta, GA, USA, and the Technical University of Munich, Munich, Germany. Since 2015, he has been with Monash University, Clayton, VIC, Australia, where he is currently a Professor and the Director of the Grid Innovation Hub. His research interests include control of power electronics systems, applications of power electronics in power and traction systems, and grid integration of renewable energy resources.

MOHAMMADREZA F. M. ARANI (Member, IEEE) received the M.Sc. degree in electrical engineering from the University of Waterloo, Waterloo, Canada, in 2012, and the Ph.D. degree in energy systems from the Department of Electrical and Computer Engineering, University of Alberta, Edmonton, AB, Canada, in 2017. From 2012 to 2013, he worked as a Research Associate with the University of Waterloo. He was an NSERC Postdoctoral Fellow with the University of Toronto, Toronto, ON, Canada, from 2017 to 2019. He joined Ryerson University, Toronto, as an Assistant Professor, in July 2019. His research interests include cyber–physical security of smart grids, renewable and distributed generation, plug-in hybrid electric vehicles, microgrids dynamics and control, and power system stability. He is the holder of the Canada Research Chair in Smart Grid Cyber–Physical Security.